



# Experimental regular and Mach reflection transition hysteresis induced by Mach-number variation and free-stream disturbances

Jacob B. Vaughn<sup>1</sup>, Edward B. White<sup>2</sup>, Ivett A. Leyva<sup>1</sup> and Rodney D.W. Bowersox<sup>1</sup>

(Received 20 August 2025; revised 15 September 2025; accepted 6 October 2025)

Hysteresis in the transition between regular reflection (RR) and Mach reflection (MR) has been predicted theoretically and numerically for decades, yet successful experimental demonstrations have remained limited to wedge-angle-variation-induced hysteresis. This work presents the first successful experimental demonstration of Mach-number-variation-induced hysteresis. Utilising a newly developed continuously variable Mach 5–8 wind-tunnel nozzle, Mach-sweep experiments were conducted on a pair of wedges at three different angles (25°, 27° and 28°). A stable RR was first established at Mach 7 within the dual-solution domain for each angle, and then the Mach number was decreased to 5. For the 27° and 28° cases, transition from RR to MR was observed at Mach 5.3 and 5.9, respectively, during the downward Mach sweep, and the MR state persisted throughout the upward sweep back to Mach 7. During the 25° case, a stable RR was maintained throughout the entire Mach sweep, prompting further experiments into the effect of free-stream disturbances on the stability of the RR state. Preliminary results revealed a free-stream-disturbance-induced hysteresis and that the RR state is metastable with potential stochastic behaviour.

**Key words:** shock waves, hypersonic flow, flow-structure interactions

### 1. Introduction

The last half-century has seen extensive research on shock wave reflection, following the foundational works of Ernst Mach (1878) and John von Neumann (1963). A central

<sup>&</sup>lt;sup>1</sup>Department of Aerospace Engineering, Texas A&M University, College Station, TX 77843, USA

<sup>&</sup>lt;sup>2</sup>Department of Mechanical Engineering, The University of Texas at Dallas, Richardson, TX 75080, USA **Corresponding author:** Jacob B. Vaughn, vaughntastic77@tamu.edu

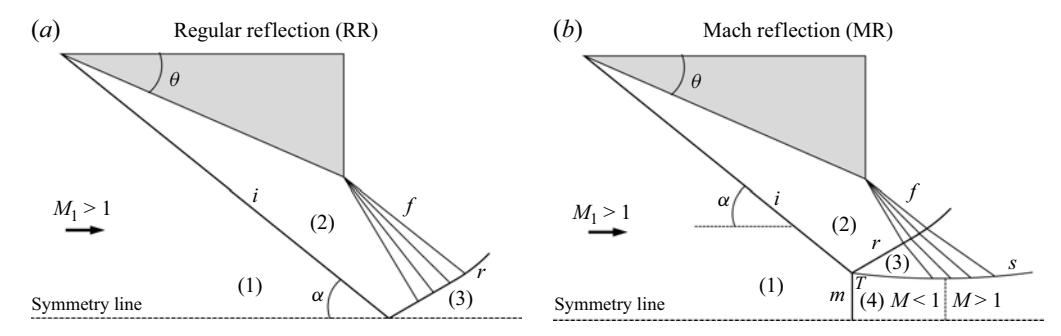


Figure 1. Schematics of shock reflection configurations: incident shock (i), reflected shock (r), Mach stem (m), trailing-edge expansion fan (f), incident-shock angle ( $\alpha$ ), slipstream (s) and triple point (T).

focus has been the transition between regular reflection (RR) and Mach reflection (MR) in steady and pseudo-steady flows (Henderson & Lozzi 1975), and the associated hysteresis predicted by Hornung, Oertel & Sandeman (1979).

In a RR (figure 1a), the incident shock (i) meets the symmetry line at a single point, where the interaction generates a reflected shock (r) that turns the post-incident-shock flow (2) back parallel to the free stream (1). In a MR (figure 1b), the oblique reflected shock is unable to turn the flow back parallel to the free stream. Instead, the incident and reflected shocks intersect at a triple point (T) located above the symmetry line. This triple point is connected to the symmetry line by a nearly vertical Mach stem (m). A slip line (s) emanates downstream from the triple point, separating the flow that has passed through the Mach stem from the flow that has passed through the incident and reflected shocks.

Both shock configurations can occur under identical free-stream conditions depending on the incident Mach number  $(M_1)$  and wedge angle  $(\theta)$ . This dual-solution domain (DSD), shown in figure 2, exists between two critical wedge-angle limits: the von Neumann condition  $(\theta_N(M))$ , below which MR is impossible, and the detachment condition  $(\theta_D(M))$ , above which RR is impossible (Ben-Dor 2007). The possibility of both shock configurations in the DSD led Hornung *et al.* (1979) to hypothesise the potential hysteresis in the RR $\rightleftharpoons$ MR transition. As evident in figure 2, there are two primary approaches to obtain the hysteresis (Ben-Dor *et al.* 2002):

- (i) Wedge-angle-variation-induced hysteresis: the flow Mach number is kept constant while the wedge angle is dynamically changed, e.g. AA'A in figure 2;
- (ii) Mach-number-variation-induced hysteresis: the wedge angle is kept constant while the flow Mach number is dynamically changed, e.g. BB'B in figure 2.

In their initial experiments, Henderson & Lozzi (1979) and Hornung & Robinson (1982) reported no evidence of wedge-angle-variation-induced hysteresis. Their results led them to conclude that the RR configuration was unstable in the DSD and that both RR $\rightarrow$ MR and MR $\rightarrow$ RR transitions occurred at the von Neumann condition. However, Teshukov (1989) later used linear stability analysis to prove that the RR configuration is stable in the DSD. This theoretical result was experimentally confirmed by Chpoun *et al.* (1995) and later by Ivanov *et al.* (2003), who successfully demonstrated both a stable RR in the DSD and a wedge-angle-variation-induced hysteresis in the RR $\rightleftharpoons$ MR transition.

While wedge-angle-variation-induced hysteresis has been demonstrated both numerically and experimentally (Mouton 2007), the alternative Mach-number-variation-induced hysteresis has only been demonstrated numerically. This was shown by Onofri &

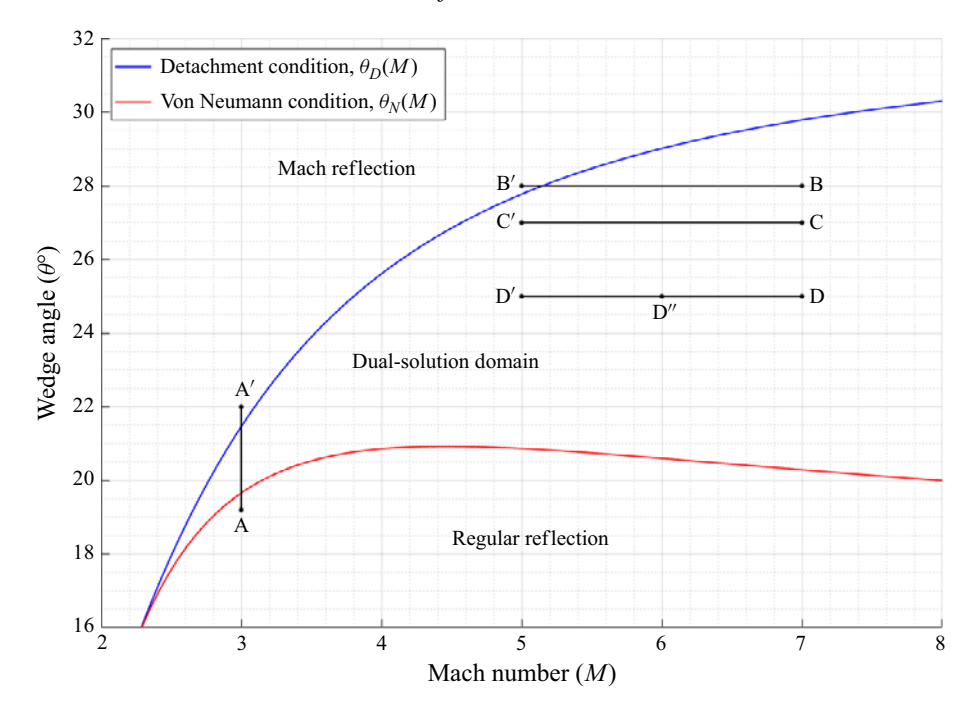


Figure 2. Dual-solution domain with hysteresis paths shown: AA'A, BB'B, CC'C, DD'D.

Nasuti (2001) and Ivanov *et al.* (2001) and was confirmed again later by Tao, Fan & Zhao (2014). Experimental attempts by Durand *et al.* (2003) and Laguarda *et al.* (2021) were unsuccessful due to free-stream disturbances (noise) present in their variable-Machnumber wind tunnels, which prevented the establishment of a stable RR within the DSD.

Additionally, the influence of wind-tunnel free-stream disturbances on the stability of the RR state was briefly explored. Previous experimental investigations by Sudani *et al.* (2002), with water vapour, and Mouton & Hornung (2008), with laser energy deposition, demonstrated that artificial disturbances can induce a RR  $\rightarrow$  MR transition. Kudryavtsev *et al.* (2002) numerically examined the threshold of density perturbations required to cause a RR  $\rightarrow$  MR transition and showed that the necessary disturbance amplitude varies throughout the DSD, decreasing as the detachment condition is approached.

The results of both previous work and the current work suggest a third dimension of the DSD and an additional transition and hysteresis mechanism, termed free-stream-disturbance-induced hysteresis, in which the Mach number and wedge angle are kept constant while finite-amplitude disturbances are introduced into the free stream.

### 2. Experimental set-up

Experiments were conducted at the Texas A&M University National Aerothermochemistry and Hypersonic Flight Laboratory (NAHL). A series of pseudo-steady Mach-sweep tests were performed using 3D-printed adjustable-angle wedge models in a blow-down

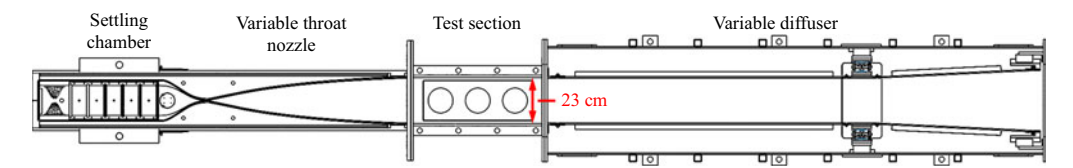


Figure 3. The ACE tunnel schematic (flow left to right); test section height shown and 36 cm width into page.

wind tunnel. High-resolution schlieren imaging was employed to visualise the resulting shock reflections.

## 2.1. Actively controlled expansion tunnel

The experiments in this work were performed using the NAHL's recently upgraded actively controlled expansion (ACE) tunnel (Tichenor *et al.* 2010; Vaughn *et al.* 2026). This conventional, cold-flow, blow-down facility features a continuously variable Mach-number nozzle, capable of dynamically testing free-stream Mach numbers over a range of 5–8. The facility supports stagnation pressures and temperatures up to 1.4 MPa and 500 K, respectively, yielding unit Reynolds numbers of  $Re' = \rho U/\mu = 0.3 - 10.0 \times 10^6 \, \text{m}^{-1}$ , with  $\rho$ , U, and  $\mu$  denoting the free-stream density, velocity, and dynamic viscosity, respectively. The run time in ACE is up to 40 s, which allows the time for pseudo-steady Mach sweeps. The test section has a height of 23 cm, a width of 36 cm and provides optical access at multiple positions along the top, bottom and sides. A schematic of ACE is shown in figure 3.

At low unit Reynolds numbers, the free-stream pressure fluctuations (noise) in ACE are  $\leq 0.1\,\%$  of the mean free-stream pressure. As the Reynolds number increases above  $3.0\times10^6~\text{m}^{-1}$  and the tunnel-wall boundary-layer transitions from laminar to turbulent, the fluctuations rise sharply to a peak of approximately 1.5 %, accompanied by a broadband increase in spectral content (Vaughn *et al.* 2026). Thus, Mach-sweep experiments in this work were conducted at a unit Reynolds number of  $1.5\times10^6~\text{m}^{-1}$  to minimise free-stream disturbances.

A few additional experiments at higher unit Reynolds numbers were conducted to explore the potential free-stream-disturbance-induced hysteresis. All experiments were conducted at a stagnation temperature of 450 K, which was sufficient to prevent oxygen liquefaction in the free stream at the tested Mach and Reynolds numbers. Additionally, the compressed air supply for ACE is passed through a regenerative desiccant air dryer to reduce the nominal dew point to 233 K prior to entering the storage tank, and the air passes through a 1  $\mu$ m filter just before entering the settling chamber. Thus, the experiments are thought to be free of phase change and particle disturbances.

# 2.2. Test article design

A pair of sharp-edged adjustable-angle wedges were 3D-printed out of Rigid 10k resin using a Formlabs Form 3L printer. The wedges were mounted symmetrically on the top and bottom of the ACE test section, as shown in figure 4(a). The wedges had a length (w) of 38 mm, span (b) of 140 mm and trailing-edge separation (2g) between 40 and 41 mm (depending on wedge angle), as illustrated in figure 4(b). These dimensions follow the aspect ratio recommendations of Fomin  $et\ al.\ (1996)$  and Skews (1997) to minimise three-dimensional edge effects, but the span is also short enough to avoid effects from the tunnel-wall boundary layer. The wedge spacing was calculated following the shock geometry recommendations of Vuillon, Zeitoun & Ben-Dor (1995) and Mouton (2007) to ensure the trailing-edge expansion fan remains downstream of the RR point of reflection, as illustrated in figure 1(a).

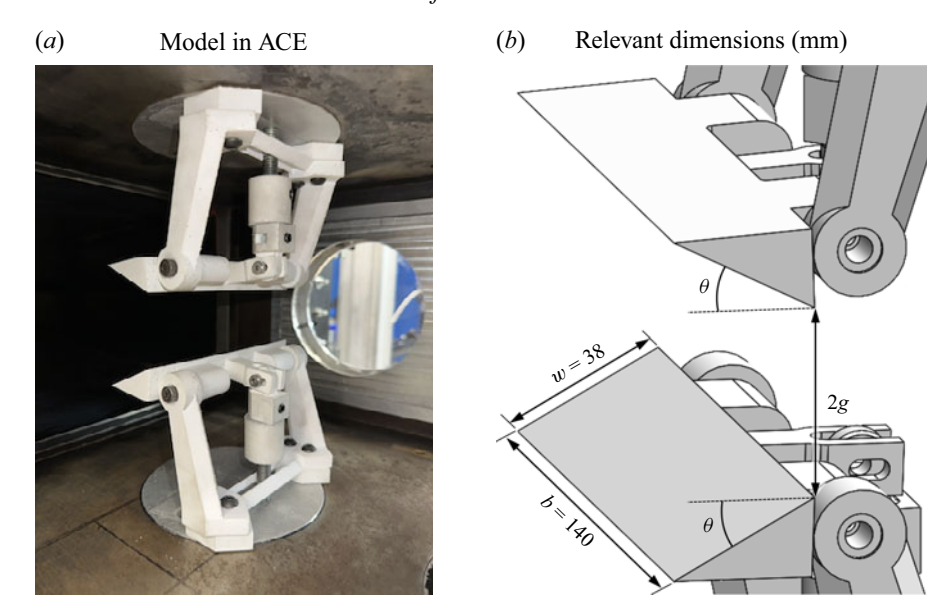


Figure 4. Experimental test article.

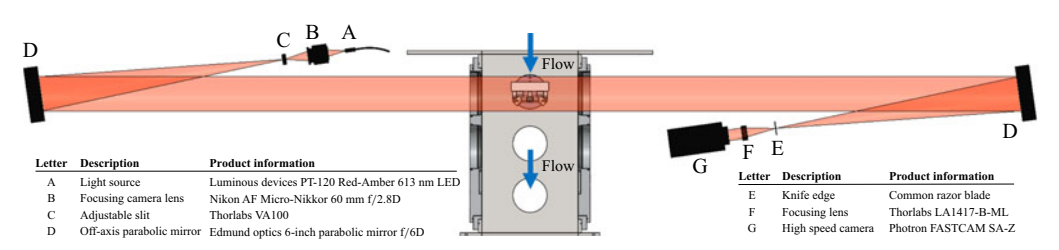


Figure 5. Schlieren set-up schematic with optical components information.

## 2.3. Schlieren imaging

Flow visualisation was performed using high-resolution z-type schlieren imaging with a continuous LED light source and a Photron FASTCAM SA-Z CMOS camera recording at 250 f.p.s. The layout and components for the schlieren set-up are shown in figure 5. The camera was synchronised with the tunnel data acquisition to enable time-resolved tracking of the shock interaction during the Mach sweeps.

### 3. Experimental results

The first set of experiments in this work followed the horizontal (Mach sweep) paths shown in figure 2:

- (i) BB'B: classical approach to obtain Mach-number-variation-induced hysteresis by crossing the detachment condition;
- (ii) CC'C: completely within DSD and approaches the detachment condition at the lowest Mach number (C') without crossing;
- (iii) DD'D: the middle of the DSD for investigating free-stream-disturbance-induced hysteresis without approaching either boundary.

A few additional experiments were conducted at point D'' in figure 2 to investigate the potential influence of free-stream disturbance levels as a third dimension of the DSD.

## 3.1. Mach-number-variation-induced hysteresis

For path BB'B, the wedges were set to  $\theta=28^{\circ}$ , as shown in figure 4(*b*), and the experiment began at Mach 7 and  $Re'=1.5\times 10^6~{\rm m}^{-1}$  to establish a stable RR within the DSD. The Mach number was then gradually decreased over a span of 8 s to Mach 5, and then increased back to Mach 7 at the same rate. A RR $\rightarrow$ MR transition occurred during the downward sweep at Mach 5.9, and the MR state persisted throughout the upward sweep without transition back to RR. Schlieren images demonstrating this hysteresis behaviour are presented in figure 6.

For path CC'C, the wedges were set to  $\theta = 27^{\circ}$ , and the same test sequence was repeated. Although not predicted theoretically, a RR $\rightarrow$ MR transition occurred during the downward sweep at Mach 5.3, and the MR state persisted throughout the upward sweep without transition back to RR. Schlieren images demonstrating this hysteresis behaviour are presented in figure 7.

The RR $\rightarrow$ MR transition in both of these experiments occurred at higher Mach numbers than predicted by the detachment condition. As reported by Chen, Bai & Wu (2020), this is likely attributed to a larger effective wedge angle due to the boundary-layer displacement thickness on the wedge surfaces. Following the theory presented by Chen *et al.* (2020), the effective wedge angles were estimated to be  $1^{\circ} \pm 0.3^{\circ}$  larger than the geometric wedge angle. This value agrees well with the approximate boundary-layer edge location and incident-shock angles measured in the schlieren images. Shifting both paths (BB'B and CC'C) in figure 2 up by  $\sim 1^{\circ}$  yields a much closer agreement between experimental and theoretical RR  $\rightarrow$  MR transition values. This correction accounts for the boundary layer on the wedges to effectively align the results with inviscid theory.

For path DD'D, the wedges were set to  $\theta=25^\circ$ , and the same test sequence was repeated again. As expected, no RR $\rightarrow$ MR transition occurred, and a stable RR was maintained throughout the entire downward and upward Mach sweep. This result reinforced that the RR state can remain stable throughout the DSD under sufficiently quiet free-stream conditions, which prompted further investigation into the role of free-stream disturbances in destabilising the RR configuration.

## 3.2. Free-stream-disturbance-induced hysteresis

Path DD'D was tested again at  $Re' = 4.5 \times 10^6 \text{ m}^{-1}$  to introduce increased free-stream disturbances, resulting in a RR $\rightarrow$ MR transition during the downward sweep at Mach 5.2 as shown in figure 8. This transition occurred in the middle of the DSD without approaching the detachment condition, suggesting that the increased free-stream disturbances sufficiently perturbed the RR state to induce the RR $\rightarrow$ MR transition.

In order to further isolate the effect of the free-stream disturbances, a few experiments were conducted with both the Mach number and wedge angle fixed at 6 and  $25^{\circ}$ , respectively (point D" in figure 2). The unit Reynolds number was swept from  $1.5 \times 10^6$  to  $5.0 \times 10^6$  m<sup>-1</sup>, increasing then decreasing, to vary the free-stream disturbances from  $\leq 0.1$ % to approximately 1.5%, respectively. This range of disturbance levels is representative of most hypersonic wind tunnels, both quiet and conventional. For a better understanding of the free-stream conditions, figure 9 shows the free-stream Mach number, unit Reynolds number and disturbance (noise) level throughout each of the runs in this work. The noise levels were measured with a Kulite high-frequency pressure

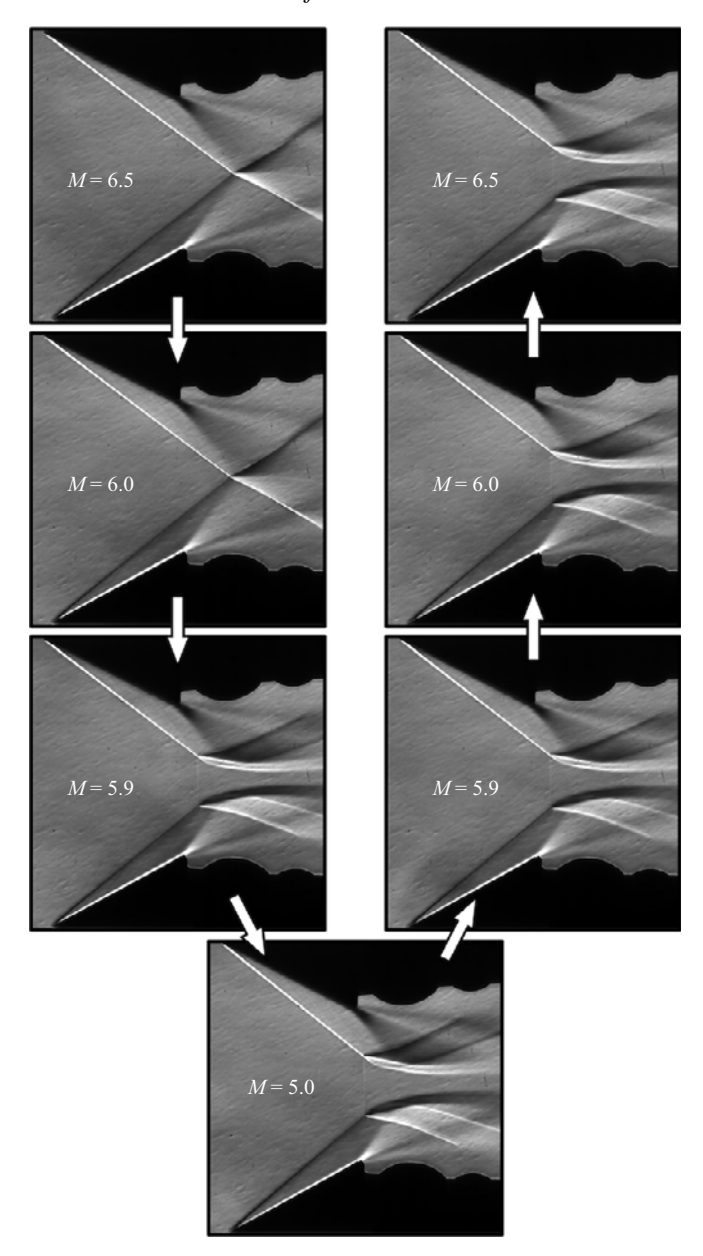


Figure 6. The RR $\rightarrow$ MR hysteresis cycle induced by Mach-number variation for  $\theta=28^{\circ}$ , 2g=41 mm and  $Re'=1.5\times 10^6$  m<sup>-1</sup> (also see Supplementary Movie 1). The dark-shaded arcs at the top and bottom of each image are parts of the wedge-angle adjustment system and do not interact with the shock waves.

transducer mounted in a Pitot tube in standalone runs following the same repeatable, programmed test sequences.

The test sequence mentioned above and shown in figure 9(c) was conducted three consecutive times with the wedges set at  $\theta = 25^{\circ}$ . Of these repeated runs, only one produced a noise-induced RR $\rightarrow$ MR transition during the high-noise portion of the cycle,

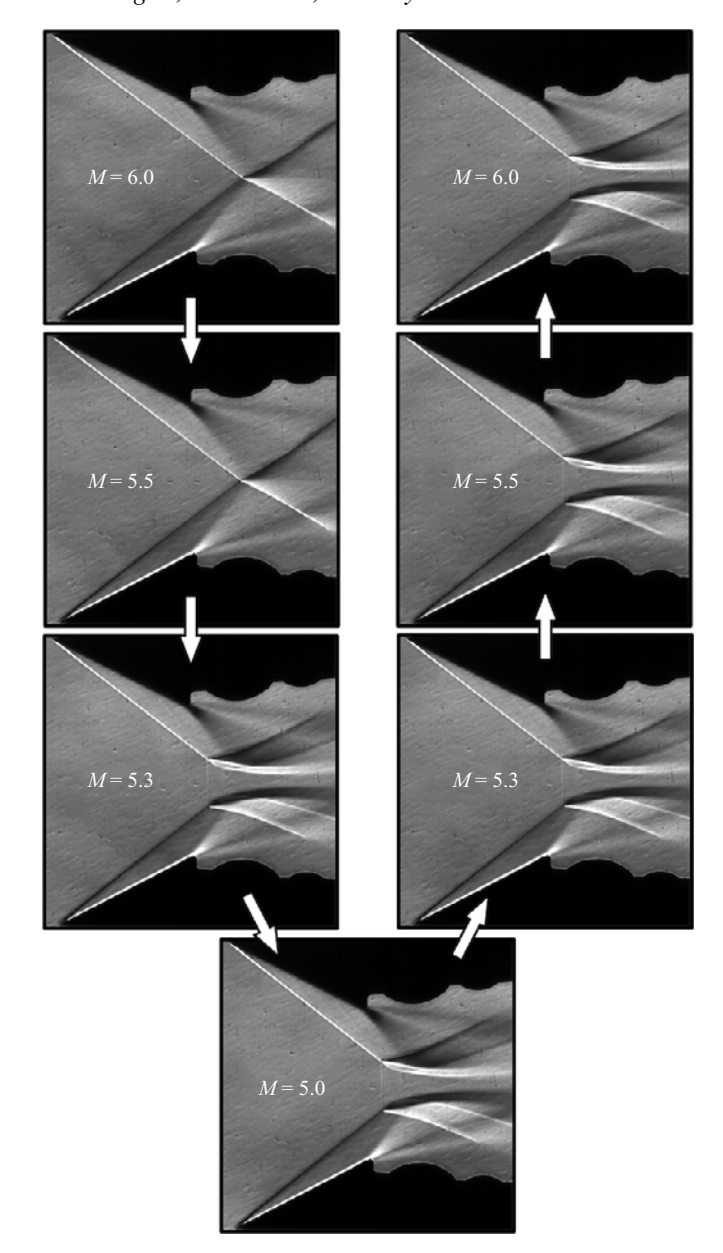


Figure 7. The RR  $\rightarrow$  MR hysteresis cycle induced by Mach-number variation for  $\theta = 27^{\circ}$ , 2g = 41 mm and  $Re' = 1.5 \times 10^6$  m<sup>-1</sup> (also see Supplementary Movie 2).

with the MR state persisting after the noise level was reduced. The other two runs maintained a stable RR throughout. Both outcomes are shown in figure 10.

While the incident-shock angle is weakly affected by viscosity via the wedge-surface boundary layer, as mentioned in § 3.1, the shock reflection behaviour is an inviscid phenomenon. Thus, the observed  $RR \rightarrow MR$  transition is attributed to the increased free-stream disturbances that ultimately destabilise the RR state; it is not due to any effect of Reynolds number. The lack of repeatability in the  $RR \rightarrow MR$  transition further supports this notion.

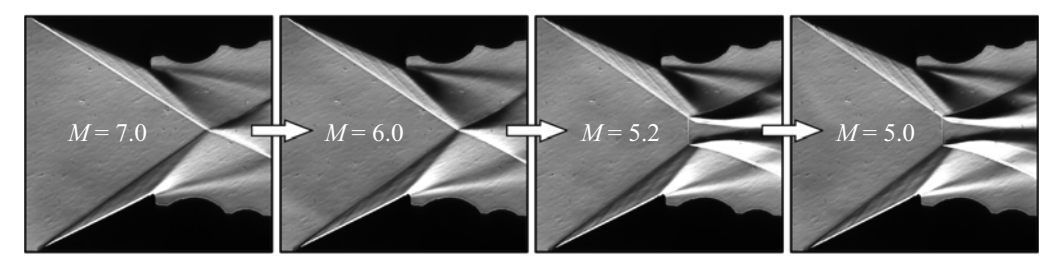


Figure 8. The RR  $\rightarrow$  MR hysteresis cycle induced by free-stream disturbances during Mach-number variation for  $\theta = 25^{\circ}$ , 2g = 40 mm and  $Re' = 4.5 \times 10^6$  m<sup>-1</sup> (also see Supplementary Movie 3).

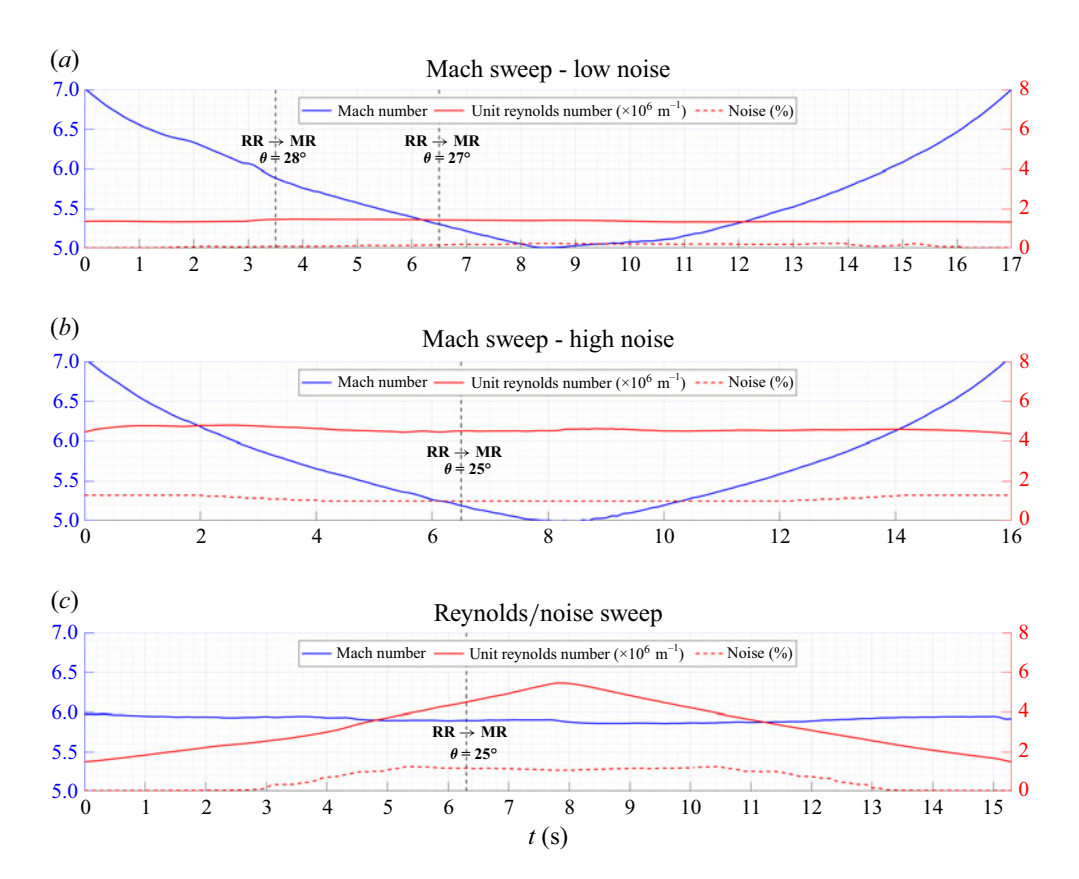


Figure 9. The ACE free-stream conditions for the various test sequences (noise calculated as  $P'_{0,rms}/\overline{P_0}$  from Pitot stagnation pressure measured with Kulite XCEL-100-5A sampled at 500 kHz and low-pass filtered at 100 kHz).

These observations suggest that the RR state within the DSD is metastable: finite-amplitude disturbances can induce a RR→MR transition. Of three repeated Reynolds-sweep experiments at fixed Mach number and wedge angle, only one produced a transition and hysteresis loop, while the other two remained in a stable RR configuration throughout. This variability implies that the transition threshold could be stochastic, likely depending on both the disturbance amplitude and its spectral content. More systematic testing with controlled disturbance inputs will be required to identify whether a repeatable threshold can be defined.

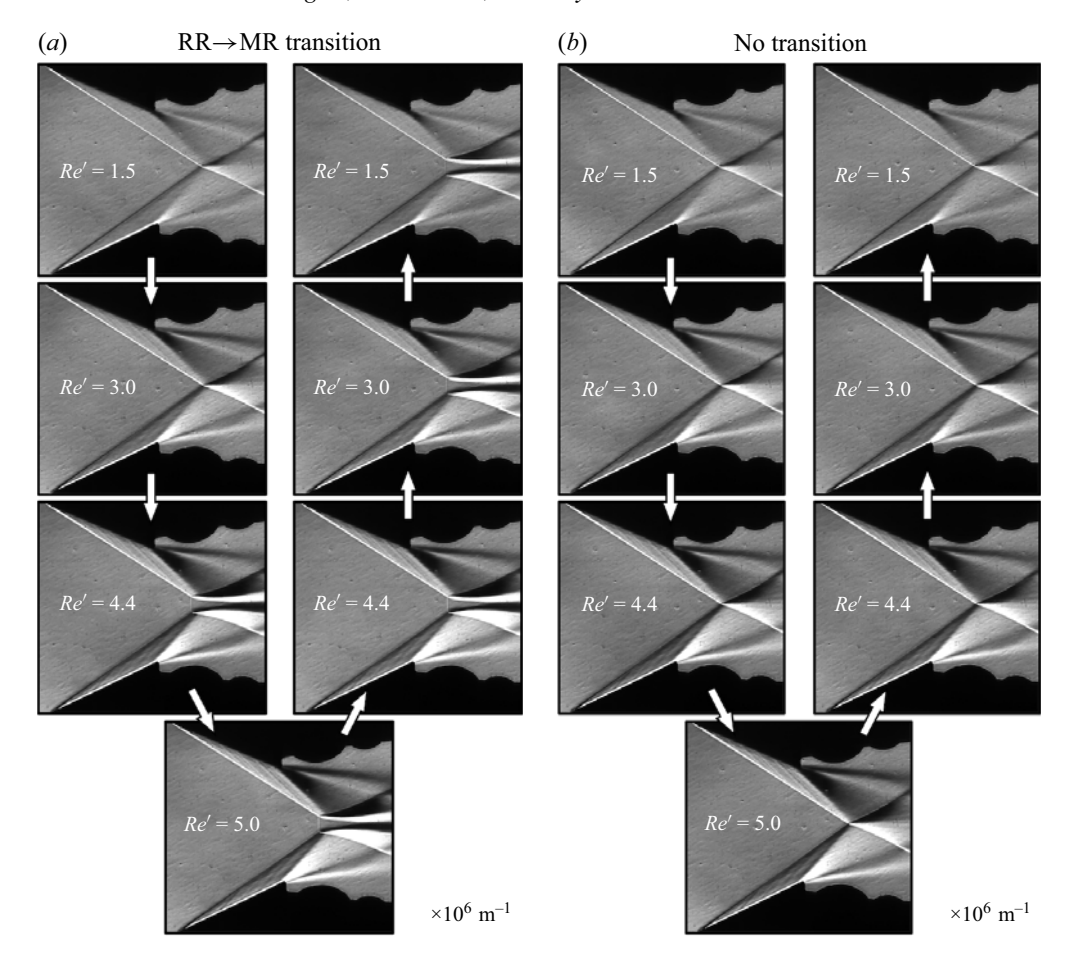


Figure 10. Both outcomes due to free-stream disturbance variations for  $\theta = 25^{\circ}$ , 2g = 40 mm and M = 6.0 (also see Supplementary Movie 4 and Supplementary Movie 5).

#### 4. Conclusions

The low-noise ( $\leq$ 0.1%) 25° test confirms that, in sufficiently quiet flow, the reflection remains regular throughout the DSD, confirming that RR is stable to small disturbances. However, the high-noise ( $\geq$ 1%) 25° results demonstrate that introducing larger disturbances can destabilise the RR state and trigger a RR $\rightarrow$ MR transition. This further suggests that the RR configuration is metastable to finite-amplitude disturbances, effectively adding a third dimension to the DSD. The inconsistent occurrence of these transitions suggests that the free-stream-disturbance-induced transition threshold may be stochastic in nature. Further experiments with controlled disturbance inputs are needed to

better quantify the critical amplitudes and spectral content responsible for this mechanism and to assess whether the transition threshold is deterministic or stochastic.

These findings validate long-standing theoretical and numerical predictions of Machnumber-variation-induced hysteresis and demonstrate that free-stream disturbances can act as an independent mechanism for transition and hysteresis. This work was made possible by the recently upgraded ACE wind-tunnel nozzle, which uniquely enables continuous Mach-number variation with low free-stream disturbances.

Supplementary movies. Supplementary movies are available at https://doi.org/10.1017/jfm.2025.10803.

Acknowledgements. The authors acknowledge the support of the staff and students at the Texas A&M NAHL.

Declaration of interests. The authors report no conflict of interest.

#### REFERENCES

- BEN-DOR, G. 2007 Shock Wave Reflection Phenomena, vol. 2. Springer.
- BEN-DOR, G., IVANOV, M., VASILEV, E.I. & ELPERIN, T. 2002 Hysteresis processes in the regular reflection ↔ Mach reflection transition in steady flows. *Prog. Aerosp. Sci.* 38 (4–5), 347–387.
- CHEN, Z., BAI, C. & Wu, Z. 2020 Mach reflection in steady supersonic flow considering wedge boundary-layer correction. *Chinese J. Aeronaut.* **33** (2), 465–475.
- CHPOUN, A., PASSEREL, D., LI, H. & BEN-DOR, G. 1995 Reconsideration of oblique shock wave reflections in steady flows. Part 1. Experimental investigation. J. Fluid Mech. 301, 19–35.
- DURAND, A., CHANETZ, B., BENAY, R. & CHPOUN, A. 2003 Investigation of shock waves interference and associated hysteresis effect at variable-Mach-number upstream flow. Shock Waves 12 (6), 469–477.
- FOMIN, V.M., HORNUNG, H.G., IVANOV, M.S., KHARITONOV, A.M., KLEMENKOV, G.P., KUDRYAVTSEV, A.N. & PAVLOV, A.A. 1996 The study of transition between regular and mach reflection of shock waves in different wind tunnels. In *Proc. 12th Int. Mach Reflection Symposium*. *Pilanesberg, South Africa*, pp. 137–151.
- HENDERSON, L.F. & LOZZI, A. 1975 Experiments on transition of Mach reflexion. J. Fluid Mech. 68 (1), 139–155.
- HENDERSON, L.F. & LOZZI, A. 1979 Further experiments on transition to Mach reflexion. *J. Fluid Mech.* **94** (3), 541–559.
- HORNUNG, H.G., OERTEL, H. & SANDEMAN, R.J. 1979 Transition to Mach reflexion of shock waves in steady and pseudosteady flow with and without relaxation. *J. Fluid Mech.* **90** (3), 541–560.
- HORNUNG, H.G. & ROBINSON, M.L. 1982 Transition from regular to Mach reflection of shock waves Part 2. The steady-flow criterion. J. Fluid Mech. 123, 155–164.
- IVANOV, M.S., BEN-DOR, G., ELPERIN, T., KUDRYAVTSEV, A.N. & KHOTYANOVSKY, D.V. 2001 Flow-mach-number-variation-induced hysteresis in steady shock wave reflections. *AIAA J.* **39** (5), 972–974.
- IVANOV, M.S., KUDRYAVTSEV, A.N., NIKIFOROV, S.B., KHOTYANOVSKY, D.V. & PAVLOV, A.A. 2003 Experiments on shock wave reflection transition and hysteresis in low-noise wind tunnel. *Phys. Fluids* **15** (6), 1807–1810.
- KUDRYAVTSEV, A., KHOTYANOVSKY, D., IVANOV, M.S., HADJADJ, A. & VANDROMME, D. 2002 Numerical investigations of transition between regular and Mach reflections caused by free-stream disturbances. Shock Waves 12, 157–165.
- LAGUARDA, L., SANTIAGO-PATTERSON, J., SCHRIJER, F.F., VAN OUDHEUSDEN, B.W. & HICKEL, S. 2021 Experimental investigation of shock–shock interactions with variable inflow Mach number. *Shock Waves* 31 (5), 457–468.
- MACH, E. (1878) Uber den Verlauf von Funkenwellen in der Ebene und im Raume. Sitzungsbr. Akad. Wiss. Wien 7, 819–838.
- MOUTON, C.A. & HORNUNG, H.G. 2008 Experiments on the mechanism of inducing transition between regular and Mach Rreflection. *Phys. Fluids* **20** (12), 126103.
- MOUTON, C.A. 2007 Transition between regular reflection and mach reflection in the dual-solution domain. PhD thesis, California Institute of Technology.
- ONOFRI, M. & NASUTI, F. 2001 Theoretical considerations on shock reflections and their implications on the evaluation of air intake performance. *Shock Waves* 11, 151–156.
- SKEWS, B.W. 1997 Aspect ratio effects in wind tunnel studies of shock wave reflection transition. *Shock Waves* 7 (6), 373–383.

- SUDANI, N., SATO, M., KARASAWA, T., NODA, J., TATE, A. & WATANABE, M. 2002 Irregular effects on the transition from regular to Mach reflection of shock waves in wind tunnel flows. *J. Fluid Mech.* 459, 167–185.
- TAO, Y., FAN, X., ZHAO & Y. 2014 Viscous effects of shock reflection hysteresis in steady supersonic flows. J. Fluid Mech. 759, 134–148.
- TESHUKOV, V.M. 1989 Stability of regular shock wave reflection. J. Appl. Mech. Tech. Phys. 30 (2), 189–196. TICHENOR, N., SEMPER, M., BOWERSOX, R., SRINVASAN, R. & NORTH, S. 2010 Calibration of an actively controlled expansion hypersonic wind tunnel. In 27th AIAA Aerodynamic Measurement Technology and Ground Testing Conference.
- VAUGHN, J., WHITE, E., LEYVA, I. & BOWERSOX, R. 2026 Design and characterization of an actively-controlled hypersonic wind-tunnel nozzle. In *AIAA 2026 SCITECH*. Forum. Accepted.
- Von Neumann, J. 1963 Oblique Re•flection of Shocks. Navy Dept. Explosive Research Rept. 12, Bureau of Ordnance, Washington, DC (reprinted in Collected Works of J. von Neumann, vol. 6, Pergamon, Oxford, 1963, pp. 238−299).
- VUILLON, J., ZEITOUN, D. & BEN-DOR, G. 1995 Reconsideration of oblique shock wave reflections in steady flows. Part 2. Numerical investigation. *J. Fluid Mech.* **301**, 37–50.